REPORT DOCUMENTATION PAGE

Public reporting burden for this collection of information is estimated to average 1 hour per response, including the time for reviewing instructions, searching existing data sources, gathering and maintaining the data needed, and completing and reviewing this collection of information. Send comments regarding this burden estimate or any other aspect of this collection of information, including suggestions for reducing this burden to Department of Defense, Washington Headquarters Services, Directorate for Information Operations and Reports (0704-0188), 1215 Jefferson Davis Highway, Suite 1204, Arlington, VA 22202-4302. Respondents should be aware that notwithstanding any other provision of law, no person shall be subject to any penalty for failing to comply with a collection of information if it does not display a currently valid OMB control number. **PLEASE DO NOT RETURN YOUR FORM TO THE ABOVE ADDRESS.**

1. REPORT DATE (DD-MM-YYYY)	2. REPORT TYPE	3. DATES COVERED (From - To)
15-05-2007	Final	01-01-2004 – 31-12-2006

4. TITLE AND SUBTITLE
SURFACE/FLUID INTERACTIONS IN MICRO & NANO-CHANNELS

5a. CONTRACT NUMBER

5b. GRANT NUMBER
FA9950-~~●~~ 04-1-0106

5c. PROGRAM ELEMENT NUMBER

6. AUTHOR(S)
Carl D. Meinhart

5d. PROJECT NUMBER

5e. TASK NUMBER

5f. WORK UNIT NUMBER

7. PERFORMING ORGANIZATION NAME(S) AND ADDRESS(ES)

University of California -
Santa Barbara
Dept. of Mechanical
Engineering
Santa Barbara, CA 93106

8. PERFORMING ORGANIZATION REPORT NUMBER

9. SPONSORING / MONITORING AGENCY NAME(S) AND ADDRESS(ES)

AFOSR
875 N Randolph St
Arlington VA 22203
Rhett Jeffries

10. SPONSOR/MONITOR'S ACRONYM(S)

11. SPONSOR/MONITOR'S REPORT

12. DISTRIBUTION / AVAILABILITY STATEMENT
Distribution A: For Public Release

AFRL-SR-AR-TR-07-0202

13. SUPPLEMENTARY NOTES

14. ABSTRACT

This research project investigates the dynamics of surface/fluid interactions that occur in micro- and nano-channels. For example, micron-resolution particle image velocimetry (micro-PIV) results suggest that a hydrophilic fluid flowing over a solid hydrophobic surface in micro- and nano-channels can create slip flow whereby the no-slip boundary condition may not be valid. The slip flow may be a result of a low-viscosity nanoscale gaseous layer forming between the fluid and the microchannel surface.

The microscale allows for free-surfaces to be controlled by surface tension. The free-surface fluidic architecture can be combined with Surface-Enhanced Raman Spectroscopy (SERS) to allow the real-time profiling of atmospheric species and detection of airborne agents. The system has been used to detect 4-aminobenzenethiol, a chemical species similar in size and structure to trinitrotoluene (TNT).

15. SUBJECT TERMS

16. SECURITY CLASSIFICATION OF:			17. LIMITATION OF ABSTRACT	18. NUMBER OF PAGES	19a. NAME OF RESPONSIBLE PERSON
a. REPORT	b. ABSTRACT	c. THIS PAGE		14	Carl Meinhart
					19b. TELEPHONE NUMBER (include area code) 805-893-4563

SURFACE/FLUID INTERACTIONS IN MICRO & NANO-CHANNELS
AFSOR FA9950-04-0106

Carl D. Meinhart
Department of Mechanical Engineering
University of California, Santa Barbara

Research Objectives

The objectives of this research project were to investigate the surface/fluid interaction in micro & nano channels that occur in a variety of situations. For example, micron-resolution particle image velocimetry (micro-PIV) results suggest that a hydrophilic fluid flowing over a solid hydrophobic surface in micro- and nano-channels can create slip flow whereby the no-slip boundary condition may not be valid. The slip flow may be a result of a low-viscosity nanoscale gaseous layer forming between the fluid and the microchannel surface.

The small length scales associated with microfluidic devices, allows surface tension to be a dominating force in microchannels. As a result, a novel microfluidic remote-sensing chemical detection platform has been developed for real-time sensing of airborne agents. This platform can potentially be adapted to micro air vehicles for broad sensing applications. The key enabling technology is a newly developed invention termed *Free-Surface Fluidics (FSF)*, where one or more fluidic surfaces, confined by surface tension forces, are exposed to the surrounding atmosphere. The free-surface architecture provides a new paradigm for the micro/nanofluidics research community.

The free-surface fluidic architecture can be combined with Surface-Enhanced Raman Spectroscopy (SERS) to allow the real-time profiling of atmospheric species and detection of airborne agents. The system has been used to detect 4-aminobenzenethiol, a chemical species similar in size and structure to trinitrotoluene (TNT).

Status of Effort

We have completed a study on the effects of absolution pressure of slip that occur in hydrophobic microfluidic channels. The slip decreases with increasing absolute pressure. In addition, we have developed the first work free-surface microfluidic channel apparatus. This information will be useful in designing computer simulation tools and microchannel flows for bio-sensors.

The free-surface flow has been tested using Quantum Nanospheres. Surprisingly, a parabolic velocity profile was present. This is the subject of on-going investigation. We have coupled the free-surface system with Surface-Enhanced Raman Spectroscopy (SERS) to detect airborne explosives. We have successfully demonstrated the ability to detect DNT, TNT, RDX, TATP, picric acid in vapor form at room temperature.

Air Force Relevance

The Air Force is interested in placing small bio-chemical sensors on unmanned air vehicles and micro air vehicles. These sensors will be used for chemical and biological warfare detection. Because of the size and weight constraints, microfluidic technology will play a key role in their development. To meet this desire, an inexpensive platform for real time monitoring of airborne chemical and biological agents has been developed. We have used this instrument to detect explosives and toxic chemicals, such as detect 4-aminobenzenethiol, a chemical species similar in size and structure to trinitrotoluene (TNT).

New Findings
Introduction to Hydrophobic Slip

The current development of microfluidic devices for micro-total analysis systems has led to research focused on fluid flow at the microscale. Since the surface to volume ratio depends inversely on the characteristic length-scale, the importance of boundary conditions increase as the dimensions of microfluidic devices decrease. For nearly a hundred years, scientists and engineers have assumed no-slip for fluid flow over a solid surface. While this assumption has been proven experimentally at the macroscale, recent experiments with micro- and nano-scale flows indicate the proper boundary condition depends both on the characteristic length-scale of the flow and the chemical and physical properties of the solid surface.

Previous experiments with hydrophobic surfaces have indicated the presence of fluid slip[i,ii,iii,iv,v,vi]. While observations of fluid slip continue to expand, the generating mechanism responsible for fluid slip is not well understood. Recently, nano-bubbles on hydrophobic surfaces were observed experimentally by Tyrell and Attard[vii] and Steitz et.al.[viii]. Lum et. al[ix] and others[x] suggest a depleted water region or vapor layer develops for water near a hydrophobic surface. Zhu and Granick indicate the calculated slip lengths at higher shear rates are consistent with a two-layer fluid model with a lower viscosity layer near the surface. However, a detailed characterization is not provided. More recently, Granick et.al.[xi] saturated tetradecane with carbon dioxide and argon and calculated the slip in a surface force apparatus with a mica and apartially wetting methyl-terminated surface. They observe no-slip behavior when tetradecane is saturated with carbon dioxide, while massive deviations from the no-slip prediction exists for tetradecane saturated with argon. They attribute this difference to the enhanced segregation of argon with the amount of segregation dependent on the material properties of the fluid, the chemical nature of the wall, and chemical identity of the dissolved gasses. This is within the context of dissolved gasses forming a vapor layer or low density region near the surface. De Gennes predicts slip lengths of order 10μm that are independent of gas layer thickness when rarefied gas conditions exist.

Tretheway and Meinhart developed an analytical model to quantify the effects an air gap has on fluid flow between two infinite parallel plates. The model shows that the slip length is highly dependent on the physical properties (viscosity and thickness) of the gas layer. The chemical composition of dissolved gasses directly affects these physical properties. For instance, at 300K, the viscosity of air is 18.6μPa s while the viscosity of carbon dioxide is 15.0μPa s. If the thickness of the gas layer is the same, a decrease is gas viscosity should increase the measured fluid slip. However, it is not readily apparent

that the gas layer thickness should remain constant for dissolved gasses with different chemical composition. As suggested by Granick et.al., the chemical nature of the dissolved gasses, of the fluid, and of the surface properties control the segregation of dissolved gasses at a surface. Thus, the chemical composition of the dissolved gas may either increase or decrease the gas layer thickness depending on its affinity to the wall and to the fluid. Gasses with a high affinity to water should display a lower slip than gasses with a low affinity to water. This work explores the proposed mechanism of Tretheway and Meinhart by measuring velocity profiles and calculating slip lengths for solutions with different dissolved gasses. In addition it further validates the effects of absolute pressure.

Hydrophobic Slip Results

Velocities were measured by micron-resolution particle image velocimetry (μ-PIV) in 30μm deep by 300μm wide extruded glass microchannels trimmed to a length of 8.25cm. Measurements were made 4 to 4.5cm from the edge to eliminate possible entrance effects and to ensure a fully developed flow profile. Deionized water seeded with 300nm fluorescent particles was injected into the channel by a gravity feed system at a flow rate of approximately 200μl/hr. Hydrophobic microchannels are created by coating the walls with octadecyltrichlorosilane (OTS). The smooth and robust monolayer is approximately 2.3nm thick with a roughness of 2-3 angstroms. The OTS layer thickness is less than 1/10000th the depth of the microchannel. Two images separated by 100-200μs were captured on a cooled, interline CCD camera and analyzed with PIV software developed by Steve Wereley (currently at the Dept. of Mechanical Eng., Purdue University). The interrogation region is 128 x 8 pixels (streamwise to spanwise), which yields a spatial resolution of 14.7x0.9x1.8μm with velocity measurements obtained to within 450nm of the wall. The out of plane measurement depth is approximately 1.8μm. To increase signal-to-noise, 110 image pairs are cross correlated. The resulting correlation functions are then averaged before peak detection, following the algorithm given by Meinhart et. al.[16]

Velocity measurements are taken near the mid-plane of the channel (13μm from the bottom) along the side wall. The field of view is aligned such that a section of the wall is included in each image. Since there are no particles in the wall, the resulting correlations for that region produce erroneous velocity vectors with magnitudes and directions that are inconsistent with the known direction of flow. The wall location is then set at the point at which the velocity vectors are erroneous. The uncertainty of the wall location is approximately 110nm.

To control the composition of dissolved gasses, the gravity flow system contains four parallel flow lines that join at the microchannel entrance. Each line can be closed independently allowing only flow from one fluid reservoir. The reservoirs are filled with particle-water solutions that have been saturated with a given gas. To saturate the solutions with a desired gas, the solutions are first degassed by applying a vacuum, pressurized with the desired gas, degassed a second time, and finally pressurized to the atmospheric with the desired gas. The saturated solutions are then transferred to the

parallel flow lines while minimizing contact with the surrounding air. The slip length is measured for each solution flowing through the same microchannel at the same location.

Table 1 provides preliminary results of the measured slip lengths obtained for two hydrophobic microchannels with saturated solutions of air, argon, and carbon dioxide in channel A and saturated solutions of air, argon, carbon dioxide, and helium for Channel B. For channel A, the results show that the slip lengths are greatest for argon, less for air, and lowest for carbon dioxide. For channel B, the slip length is greatest for helium, slightly less for argon, lower still for air, and essentially zero for carbon dioxide. The results suggest that the nature of the dissolved gas affects the properties of the gas layer that develops at the hydrophobic wall. However, the chemical composition of gas manifests its effects through more than a difference viscosity. From the proposed mechanism of Tretheway and Meinhart[9] the slip should depend inversely on the gas layer viscosity. If we compare the results of Table 1 for argon and helium (two Noble gasses) in channel B, we see that the measured slip length of helium is 1.12 times that of argon. The viscosity ratio of argon to helium is 1.145. Since the slip length depends inversely of the viscosity, the results of helium and argon are consistent with sole effect of viscosity. While the viscosity ratio seems to hold true for a comparison and helium and argon, Table 1 shows that the measured slip length is smallest for the lowest viscosity gas, carbon dioxide and greatest for the largest viscosity gases, argon and helium. This indicates that a difference in viscosity is not the sole effect that results from a different

Channel	Dissolved Gas	β (nm)	Viscosity (μPa s)
A	air	381.5	18.6
A	argon	443.6	22.9
A	carbon dioxide	233.4	15.0
B	air	175.8	18.6
B	argon	322.5	22.9
B	carbon dioxide	-4.47	15.0
B	helium	361.5	20.0

Table 1. Measured slip lengths in two hydrophobic microchannels (A and B) for various dissolved gasses. For reference the viscosity of each gas is provided.

chemical composition of the dissolved gas. The reduced viscosity of carbon dioxide must be counteracted by concurrent reduction in the gas layer thickness. This reduction in gas layer thickness may develop from the substantially greater solubility of carbon dioxide in water than either argon or helium in water. The solubility of carbon dioxide in water is 7.07×10^{-4} mole fraction, the solubility of helium 7.044×10^{-6} mole fraction, and the solubility of argon is 2.748×10^{-5} mole fraction. Thus, argon and helium may preferentially segregate from water at the hydrophobic interface. Further work with a larger array of gasses with varying viscosity and solubilities needs to be conducted to fully elucidate the effects of both viscosity and solubility on the measured slip length.

Figure 1 shows the measured slip length (previously reported) as a function of absolute pressure for a hydrophobic microchannel. The experimental conditions (flow rate, temperature, microchannel location, etc) remained constant regardless of absolute

pressure. Velocity profiles were measured and slip lengths calculated as the absolute pressure was increased and decreased from atmospheric to 600kpa and back to atmospheric. Figure 1 shows that as the absolute pressure increases the calculated slip length decreases to no-slip at the highest pressure. The method to determine the slip length was described previously in the experiments section. A major factor in this calculation is setting the wall location. To validate the methodology of locating the wall, an alternate method to examine the velocity profiles was applied. This method employs the nanoscope technique of Stone[17]. It calculates the wall position by fitting the velocity data with a second order polynomial and locating the point at which the velocity goes to zero. The results show that as the pressure increases, the wall location increases. This is consistent with a reduction in fluid slip. If we set the wall position to correspond to the highest pressure and subtract this from the wall position at lower pressures, the slip lengths at lower pressures may be calculated. Applying this method produces slip lengths consistent with those shown in Fig. 1. This further validates the previously reported absolute pressure effects and methodology to identify the wall location.
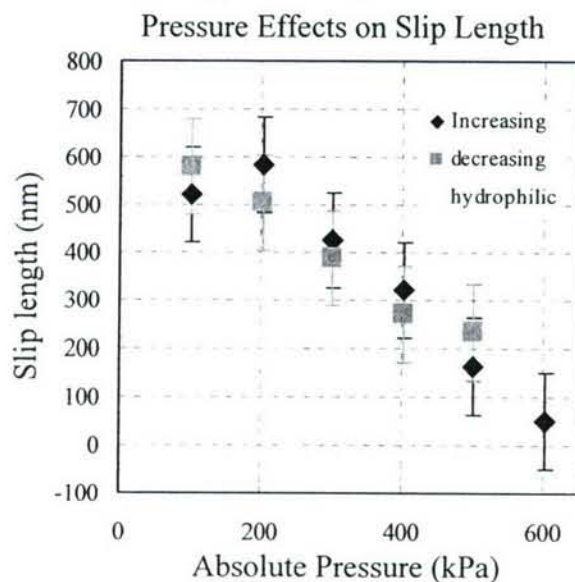

Figure 1: *The effects of absolute pressure on the measured slip length.*

Free-Surface Fluidics
For the first time, an integrated nanoscale fluidic platform has been developed that can monitor airborne agents in real time. During the past fifteen years, there has been significant development in using micro/nanofluidic-based platforms for detection of chemical and biological agents. However, no integrated device currently exists for capturing airborne agents and injecting them into a microchannel. This is a longstanding barrier that could ultimately limit the viability of 'lab on a chip' platforms for monitoring of airborne species.

The key breakthrough that makes the new system possible is the invention of *Free-Surface Fluidics*[xii] *(FSF)* which leverages new physical phenomena. Free-surface fluidics has not been demonstrated previously in micro/nanofluidic platforms and enables absorption of airborne chemical agents directly into the fluidic channels. This

advancement constitutes a significant step towards real-time sensing of airborne biological and chemical agents, with applications to environmental monitoring and biowarfare detection that significantly enhances what is achievable with conventional lab-on-a-chip platforms[xiii,xiv,xv].

A schematic of the FSF architecture is shown in Fig. 2. The microfluidic device consists of a 3-sided microchannel, with the top being exposed to the atmosphere. When water is present in the microchannel, the surface tension of the free surface confines the fluid to the channel, and allows for pressure-driven flow through the channel. In addition, the free surface allows airborne molecules to be absorbed directly into the working fluid. The working fluid and its chemical constituents can be imaged by a microscope lens. Figure 3 shows an open channel that was microfabricated from a silicon wafer.
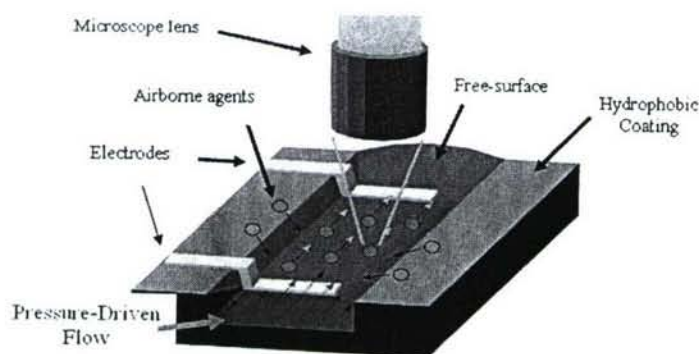

Figure 2: *Free-surface micro/nanofluidic platform. Surface tension is a dominant force at the micron and sub-micron length scales. The surface tension force can create significant pressure gradients that can drive the flow and maintain stability of the free surface. Here, electrodes on the substrate can be used for a variety of purposes, such as virtual valves, low-voltage electrophoretic separation, and electro-osmotic flow. A microscope lens will be used for detection by surface-enhanced Raman spectroscopy. The free-surface allows for direct absorption of airborne chemical agents directly into the working fluid.*

Figure 3: *Image of silver colloid flowing through an 18-micron wide free-surface microchannel. The top surface of the flow is exposed to the atmosphere and provides a prototype platform for remote sensing of airborne agents by SERS.*

Pressure-driven flow in this channel has been measured using micron Particle Image Velocimetry (micro-PIV). We have developed a new type of flow-tracing particle (termed Quantum Nanosphere) to measure fluid velocity in sub-micron channels. A schematic of a Quantum Nanosphere is shown in Fig. 4. In one instance, the velocimetry results indicate a ~0.1 mm/s flow with a peaked velocity profile (see Fig. 5). Other experiments have established that liquid velocities ~ 1 mm/sec can be established in open channels ~ 1 μm deep. When the open channel connects to reservoirs (either closed or open), the free surface can be kept clean from monolayers because of the relatively short transit time during which the liquid is exposed to the atmosphere. Nonetheless, the airborne agents will diffuse through submicron-depth layers in time scales ~ 10^{-2} sec, assuming typical diffusivities of ~10^{-6} cm^2/sec. Evaporation from such open channels can be controlled or eliminated, as required, by controlling the temperature of the liquid

in the open channel. This can be done by using the Peltier effect to keep the fluid close to the dew point of the surrounding air. We have demonstrated this technology. In some situations, a controlled amount of evaporation may be desirable in order to concentrate the absorbed species, making detection easier. In such cases, the temperature of the liquid can be allowed to rise somewhat above the dew point, and the amount evaporated determined by measuring the axial concentration profile of a non-volatile species dissolved in the liquid that serves as a marker. The concentration of such markers and absorbed airborne agents can be measured with high accuracy by surface-enhanced Raman spectroscopy, allowing sensitive detection of a wide variety of chemical, biological and environmental agents.
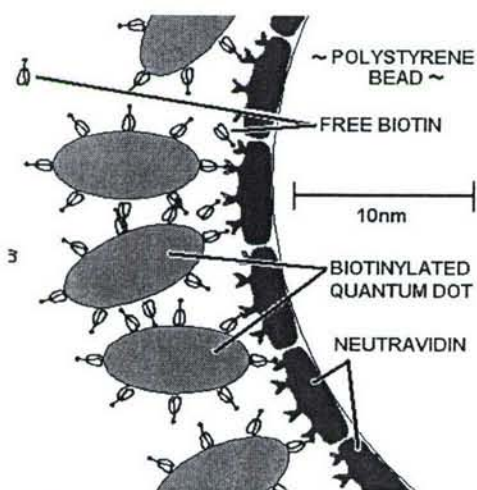

Figure 4. *Beads coated with NeutrAvidin™ were titrated into a solution containing biotinylated quantum dots. Free biotin was added after the beads were coated with QDs so remaining NeutrAvidin™ binding sites would be filled.*
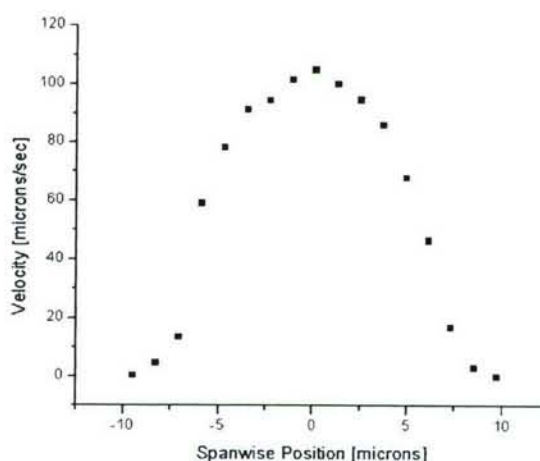

Figure 5. *Micro-PIV measurements of pressure-driven flow in a free-surface microfluidic channel. The velocity profile is peaked because of the variation in free-surface elevation. In this case, the maximum velocity is 100 um/s.*

Surface-enhanced Raman Spectroscopy (SERS) is a chemical detection technique that has been actively developed for over 25 years[xvi]. Based on the specificity and uniqueness of the Raman spectrum obtained from a particular material, SERS allows the rapid detection and identification of chemical compounds[xvii,xviii]. Surface enhancement of Raman spectra is obtained from the coupling of an analyte with nanostructured materials which are designed to concentrate the electromagnetic fields associated with surface plasmon resonance. Now a mature analytical technique, the SERS effect is observed to enhance Raman spectra of analyte materials up to 10^{11} times[xix]. This allows the routine detection of a single analyte molecule and is one of the most sensitive chemical detection techniques yet discovered.

As of now, the SERS technique is confined to the detection of materials suspended in liquid solution. We have, for the first time, developed a method to detect gas-borne materials by coupling the sensitivity of SERS chemical detection with our Free Surface Microfluidic Platform (see Fig. 6). This combination produces a highly sensitive, real-time gas-phase chemical sensor which relies on the small vertical dimension and

uncovered top surface of the liquid flow in the microfluidic platform to quickly equilibrate a solution of nanoscale silver colloid solution with the surrounding atmosphere.

In preliminary studies, a free-surface flow of silver colloid was established in a microchannel of dimensions 18um wide by 10mm long by 1.5um deep. A liquid solution of 4-aminobenzenethiol was placed approximately 3cm from the microchannel that contained the flow of silver colloid (Fig. 6). The microchannel and 4-aminobenzenethiol were placed inside a 20cm x 20cm x 0.6cm box in order to contain the 4-aminobenzenethiol vapor. Raman spectroscopy was then performed in the center of the microchannel with a 514.5 nm, 7 mW laser through a 1000 microscope.

The Raman spectrum results are shown in Fig. 7. After only 5 seconds of exposure the characteristic signature of 4-aminobenzenethiol is readily apparent. This chemical was chosen because its molecular structure is similar to TNT.
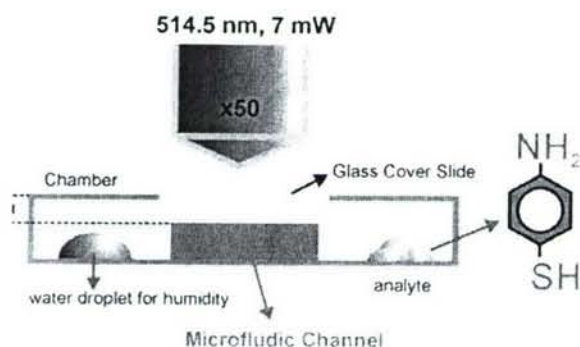

Figure 6: Schematic of our prototype microchannel SERS platform. A free-surface microchannel flow of silver colloid was established in an atmosphere which was exposed to solid 4-aminobenzenethiol (analyte). Analyte contacted the free-surface flow by diffusion through the atmosphere and subsequently adsorbed to the suspended silver colloid.
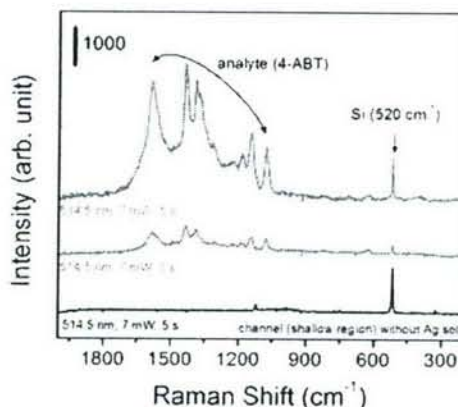
Figure 7: Characteristic Raman peak detection of 4-aminobenzenethiol after 1s and 5s of signal integration time obtained by our prototype microchannel SERS platform (red traces). The analyte had diffused through the atmosphere and adsorbed to the silver colloid in order to produce the SERS signal. In absence of analyte, no peaks between 1000-1700cm-1 were detected (black trace).

Explosives Vapor Detection
Figure 8 shows the integrated free-surface microfluidic platform combined with SERS for molecular-specific detection. The free-surface flow utilizes surface tension to create pressure-driven flow. Once absorbed in the fluid in the microfluidic channel, the airborne molecules or particles adsorb on the silver nanoparticles, causing them to aggregate. This leads to a greatly-enhanced SERS effect. As the particles advect downstream, colloidal particles continue to aggregate: monomers form dimers, and dimers form trimers, etc. A confocal Raman system can probe the free-surface channel anywhere along the stream and can therefore select the streamwise position where the maximum concentration of dimers are present. This allows us to measure a wide variety of explosive vapors,

including DNT, TNT, picric acid, TATP and RDX under highly reproducible conditions of nanoparticle aggregation, and hence SERS enhancement. The system is also capable of measuring explosive particles.
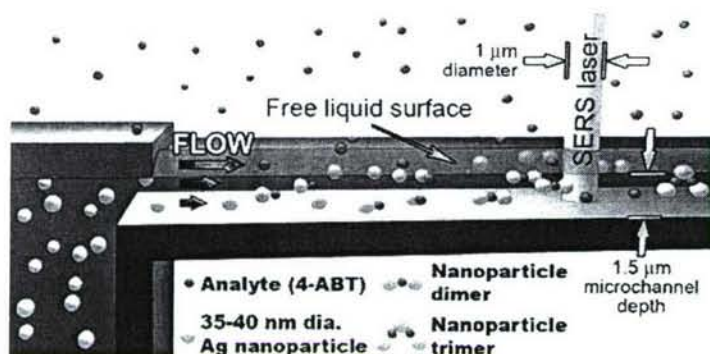

Figure 8: Free-surface microfluidic platform. Surface tension is a dominant force at the micron length scales. The surface tension forces can create significant pressure gradients that drive the flow and maintain stability of the free surface. The free-surface allows for direct absorption of airborne chemical agents directly into the aqueous working fluid. The absorbed molecules aggregate the Ag colloidal particles to create the SERS effect. As the particles advect downstream, colloidal aggregation increases. The maximum SERS signal is obtained from nanoparticle dimers.

Figure 9 is a picture of the free-surface microfluidic chip on a temperature-controlled confocal Raman microscope stage. With this system, we have successfully measured vapor of DNT, TNT, TATP, picric acid, and RDX at room temperature. Typical SERS spectra are shown in Fig. 10 (TATP spectrum not shown). The spectrum of each molecule is distinct and clearly shows the characteristic NO_2 stretch near 1400 cm^{-1}.

Figure 9. Confocal Raman microscope stage with a Peltier junction for temperature control. The free-surface microfluidic chip is exposed to explosives vapor and interrogated with a 1 μm dia. laser beam. The emitted spectrum is then used to determine the airborne agents.
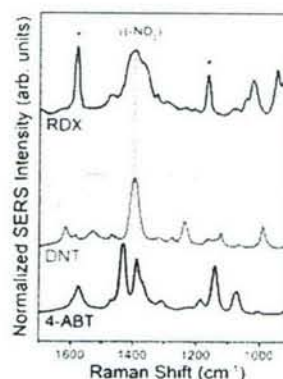
Figure 10. Surfaced-enhanced Raman spectra from explosives vapor of RDX, Picric acid, and DNT. The 4-ABT spectrum is shown for reference. Other molecules measured are TATP and TNT (Data not shown).

The saturated vapor concentrations at room temperature vary from ~10 ppb for TNT, ~10^2 ppb for DNT, to ~10^6 ppb for volatile species like TATP. The low vapor pressure of RDX makes it difficult to measure at room temperature. The saturated vapor concentration for RDX is ~10 ppt at 300 K (room temperature), and increases to ~10^2 ppb at 400 K. Therefore, all previous detections of RDX are obtained by: (1) swabbing the

sample, (2) heating the swab to ~ 400-450 K to vaporize RDX, and then (3) using a variety of techniques MS, IMS, or Fido™, etc. to obtain a measurement.

By contrast we have successfully measured RDX vapor at room temperature with our microfluidic/SERS device. The RDX test samples were obtained from *Accustandard, Inc.* (product number M-8330-05-0.1X)[xx], and certified to be 100% pure RDX sample (using HPLC) in methanol:acetonitrile solvent. Solid RDX samples were prepared by subjecting the RDX solution to an N_2 gas stream while maintaining the temperature of the solution at 25 C. This procedure evaporated the solvent, leaving pure RDX at the bottom of a test tube. The test tube was then covered with parafilm and allowed to equilibrate to room temperature for 30 minutes. The test tube was then uncovered and oriented next to the detector such that the vapor transport distance between the RDX and the detector was 5 cm.

Based on the reported vapor pressure of RDX we believe our measurements were in the ppt range. High quality spectra were obtained (see Fig. 10). We have yet to optimize the sensitivity limits of our system, and feel it is possible to increase the sensitivity significantly by improvements in optics and geometry.

Current explosives detectors and SERS-active substrates exposed to air can be degraded or spoofed by contamination from ambient chemicals such as gasoline & jet fuel vapor, shoe polish, perfume, etc. We have tested DNT in a saturated gasoline vapor environment and found no observable degradation in signal as a result of the gasoline vapor. We have also measured DNT in the presence of volatiles like ethyl alcohol and acetone, and observed only minor additional spectral features, allowing the characteristic (and dominant) spectrum of DNT to be confidently and quantitatively extracted.

Conclusions

This work examines the effects of dissolved gasses on apparent fluid slip in hydrophobic microchannels and further validated the effects of absolute pressure. The results show the measured slip lengths depend on the dissolved gasses in solution. The measure slip lengths are greatest for helium, slightly smaller for argon (which is consistent with a change in viscosity), lower still for air, and smallest (nearly zero) for carbon dioxide. The slip length measured with carbon dioxide is the smallest even though it has the lowest viscosity. This indicates that the reduced viscosity of carbon dioxide must be counteracted by a simultaneous reduction in the gas layer thickness. This reduction in gas layer thickness may develop from the substantially greater solubility of carbon dioxide in water. These results are consistent with the generating mechanism of Tretheway and Meinhart[9] as the model shows that the slip length is highly dependent on the nanobubble or gas layer. However, further work with an array of gasses is necessary to fully elucidate the effects of soluble gasses.

We have developed a new microfluidic-based platform for sensing biological and chemical agents. This platform can be used in conjunction with micro air vehicles. In this system, airborne molecules can be directly absorbed through the microfluidic free-surface for immediate detection using a number of techniques including the interaction with gold or silver colloidal particles which allows the subsequent detection by SERS. The platform is capable of detecting 4-aminobenzenethiol (a chemical similar in structure to TNT). We have demonstrated detection with only 5 seconds of atmospheric exposure.

In order to develop further this device for use with explosives detection, the microfluidics technologies will need to be developed and optimized for pressure-driven free-surface flows, free-surface valves, and evaporative pumps. We will also design further the microfluidic/SERS sensing system to be compatible with micro air vehicles for remote sensing of airborne molecules.

In order to illustrate the utility of the Free Surface Fluidics / SERS system as an explosives detector, we have measure vapor-phase of several explosive agents, including, DNT, picric acid, RDX, and TATP.

Acknowledgement/Disclaimer

References

[i] . R. Pit, H. Hervet, and L. Leger, "Direct experimental evidence of slip in hexadecane: solid interfaces". Physical Review Letters, **85**, 980 (2000).

[ii] Craig. et.al., "Shear-dependent boundary slip in an aqueous Newtonian liquid". Physical Review Letters, vol. **87**, 054504 (2002).

[iii] Y. Zhu and S. Granick, (2001), "Rate-dependent slip of Newtonian fluids at smooth surfaces". Phys. Rev. Lett. **87**, 96 (2001).

[iv] Y. Zhu and S. Granick, "Limits of the hydrodynamic no-slip boundary condition". Physical Review Letters, vol. **88**, 106102 (2002).

[v] D.C. Tretheway and C.D. Meinhart, "Apparent fluid slip at hydrophobic microchannel walls". Physics of Fluids, **14**, L9 (2002).

[vi] . C. Choi, J.A. Westin, and K.S. Breuer, "Apparent slip flows in hydrophilic and hydrophobic microchannels". Physics of Fluids **15**, 2897 (2003).

[vii] J. Tyrell and P. Attard, "Images of nanobubbles on hydrophobic surfaces and their interactions". Physical Review Letters, **87**, 176104 (2001).

[viii] R. Steitz, T. Gutberlet, T. Hauss, B. Klosgen, R. Krastev, S. Schemmel, A.C.; Simonsen, and G.H. Findenegg, "Nanobubbles and their precursor layer at the interface of water against a hydrophobic surface". Langmuir, **19**, 2409-2418 (2003).

[ix] . K. Lum, D. Chandler, and J.D. Weeks, "Hydrophobicity at small and large length scales". Journal of Physical Chemistry B., vol. **103**, 4570-4577 (1999).

[x] K. Lum, D. Chandler, and J.D. Weeks, "Hydrophobicity at small and large length scales". Journal of Physical Chemistry B., vol. **103**, 4570-4577 (1999).; M. Sakurai, H. Tamagawa, K. Ariga, T. Kunitake, and Y. Inoue, "Molecular dynamics simulation of water between hydrophobic surfaces. Implications for the long-range hydrophobic force". Chemistry Physical Letters **289**, 567-571 (1998); D. Schwendel, T. Hayashi, R. Dahint, A. Pertsin, M. Grunze, R. Steitz, and F. Schreiber, "Interaction of water with self-assembled monolayers: neutron reflectivity measurements of the water density in the interface region". Langmuir, **19**, 2284-2293 (2003).

[xi] S. Granick, Y. Zhu, and H. Lee, "Slippery questions about complex fluids flowing past solids". Nature Materials, **2**, 221-227 (2003).

[xii] Piorek, B., Meinhart, C., Banerjee, S., "Free Surface Fluidics: A Pressure Driven, Open-Surface Nanofluidic Platform Confined by Surface Tension"; article in progress.

[xiii] Blohm D., Guiseppi-Elie A., "New Developments in Microarray Technology"; Curr. Opin. Biotechnol. **12** 1, 2001.

[xiv] Lin, F., Sabri, M., Alirezaie, J., Li, D., Sherman, P., "Development of a Nanoparticle-Labeled Microfluidic Immunoassay for Detection of Pathogenic Microorganisms", Clinical and Diagnostic Laboratory Immunology, **12** 3, 2005.

[xv] Rider, T., Petrovick, M., Nargi, F., Harper, J., Schwoebel, E., Mathews, R., Blanchard, D., Bortolin, L., Young, A., Chen, J., Hollis, M.,"A B Cell-Based Sensor for Rapid Identification of Pathogens"; Science **301** 5630, 2003.

[xvi] Kneipp, K., Kneipp, H., Itzkan, I., Dasari, R., Feld, M., "Ultrasensitive Chemical Analysis by Raman Spectroscopy"; Chem. Rev. **99** 10, 1999.

[xvii] Zhang, X., Young, O., Lyandres, O., Van Duyne, R., "Rapid Detection of an Anthrax Biomarker by Surface-Enhanced Raman Spectroscopy"; J. Am. Chem. Soc. **127** 12, 2005.

[xviii] Cao, Y., Jin, R., Mirkin, C., "Nanoparticles with Raman Spectroscopic Fingerprints for DNA and RNA Detection"; Science **297** 5586, 2002.

[xix] M. Moskovits and Blanka Vlčková, Adsorbate-induced silver nanoparticle aggregation kinetics, *J. Phys. Chem. B* **109** (31): 14755-14758 (2005).

[xx] Accustandard, Inc. maintains ISO 9001:2000 and ISO 17025:1999 certifications. Accustandard laboratories are accredited by NIST/NVLAP.

Personnel Supported During Duration of Grant

Carl D. Meinhart	Professor, University of California Santa Barbara
Derek C. Tretheway	Postdoc, University of California, Santa Barbara
Brian Piorek	Graduate Student, University of California, Santa Barbara
Shannon Stone	Graduate Student, University of California, Santa Barbara
Matthew Pommer	Graduate Student, University of California, Santa Barbara
Nora Dakessian	Undergraduate Student, University of California

Publications

Piorek, B.D, Lee, S.-J., Santiago, J.G., Moskovits, M., Banerjee, S. & Meinhart, C. D. Free-surface microfluidic control of surface enhanced Raman spectroscopy for the optimized detection of airborne molecules. Submitted to *Proc. Nat. Acad. Sci.*

Bown, M.R, C. D. Meinhart 2006 AC electroosmotic flow in a DNA concentrator. *Micro and Nanofluidics*, Vol. 2, 513.

Bottausci, F., Cardonne, C., Meinhart, C., Mezic, I. 2007. An Ultrashort Mixing Length Micromixer: The Shear Superposition Micromixer, submitted *Lab on a Chip*, 7, 396 - 398.

Piorek, B., Mechler, A., Freudenthal, P., Lal, R., Meinhart, C.D., Banerjee, S.2006. Nanoscale resolution microchannel velocimetry by atomic force microscopy. Applied Physics Letters, 89, 153123..

Freudenthal, P., Pommer, M., C.D. Meinhart. 2006. Quantum Nanosperes for Sub-Micron Velocimetry, *Exp inFluids*. In Press.

Matt Pommer, Amy Song & Carl Meinhart, 2006. Measurement of Shear Stress Distribution on a Human Blood Cell, submitted to *Meas. Sci. Tech.*

Marin Sigurdson, Dazhi Wang, C. D. Meinhart, 2005. Electrothermal stirring for heterogeneous immunoassays, *Lab on a Chip*, volume 5, issue 12.

L. Zhu, L. Petzold, D. Tretheway & C. D. Meinhart 2005 Simulation of fluid slip at hydrophobic microchannel walls by the Lattice Boltzmann Method, *J. Computational Physics*, Vol. 202, No. 1, Jan. 2005, pp. 181-195.

Dazhi Wang, Marin Sigurdson & Carl Meinhart 2005 Experimental Analysis of particle and Fluid Motion in AC Electrokinetics, *Exp. in Fluids.*, Vol. 38, No. 1, pp. 1-10.

D. Tretheway & C. D. Meinhart 2004. A generating mechanism for fluids slip in a hydrophobic microchannel. *Phys. Fluids Vol. 16, No. 5 pp 1509-1515, May 2004.*

Honors and Awards Received

- Invited speaker, 1st IEEE NEMS Conference, Zhuhai, China, 2006
- Keynote speaker, 1st Comsol Multiphysics User Conference, Boston, MA, 2005
- Keynote speaker, 6th International Conference on Particle Image Velocimetry, Pasadena, CA, 2005
- Keynote speaker, 1st Workshop on Micro-Particle Image Velocimetry, Tech. Unv. of Delft, Netherlands, 2005
- Keynote speaker, International Symposium on Micro & NanoTechnology ISMNT, Honolulu, HI, 2004.

AFRL Point of Contact

Dr. Andrew Ketsdever, Edwards AFB, CA, Phone (661)-275-6245

Transitions

Micron-Resolution PIV Patent No. 6,653,651, and 7,057,198 has been licensed to *TSI, Inc.* The point of contact at TSI, Inc. is Dr. Rajan Menon, TSI, Inc., 500 Cardigan Road, Shoreview, MN 55126-3996, Phone 800-874-2811.

Device and Methods of Detection of Airborne Agents has been optioned by SpectraFluidics, LLC., 209 W. Alamar Ave, Ste. A, Santa Barbara, CA.

New Discoveries

Quantum Nanosphere technology for flow-tracing particles has been developed in conjunction with *Nanex*, LLC, Santa Barbara, CA.

C.D. Meinhart, J.G. Santiago, B. Piorek, S. Banerjee, M. Moskovits. Device and Methods of Detection of Airborne Agents, Provisional Patent.

Patents

C. D. Meinhart, J. G. Santiago, S. T. Wereley, and R. J. Adrian. Micron resolution particle image velocimeter, Patent No. 6,653,651 Issued Nov. 25, 2003.

C. D. Meinhart, J. G. Santiago, S. T. Wereley, and R. J. Adrian. Depth-of-field micron resolution velocimetry with pulsed images of injected solid particles. Patent No. 7,057,198, June 6, 2006.